

## RESEARCH ARTICLE

# Activity of AC electrokinetically immobilized horseradish peroxidase

Mareike Prüfer<sup>1</sup>  | Christian Wenger<sup>2</sup>  | Frank F. Bier<sup>3</sup> | Eva-Maria Laux<sup>1</sup> | Ralph Hölzel<sup>1</sup>

<sup>1</sup>Fraunhofer Institute for Cell Therapy and Immunology, Branch Bioanalytics and Bioprocesses (IZI-BB), Potsdam-Golm, Germany

<sup>2</sup>IHP GmbH - Leibniz Institute for Innovative Microelectronics, Frankfurt/Oder, Germany

<sup>3</sup>Institute of Biochemistry and Biology, University of Potsdam, Potsdam-Golm, Germany

## Correspondence

Mareike Prüfer, Fraunhofer Institute for Cell Therapy and Immunology, Branch Bioanalytics and Bioprocesses (IZI-BB), Am Mühlenberg 13, 14476 Potsdam-Golm, Germany.

Email:

[Mareike.Pruefer@izi-bb.fraunhofer.de](mailto:Mareike.Pruefer@izi-bb.fraunhofer.de)

**Color online:** See article online to view Figures 1–9 in color.

## Abstract

Dielectrophoresis (DEP) is an AC electrokinetic effect mainly used to manipulate cells. Smaller particles, like virions, antibodies, enzymes, and even dye molecules can be immobilized by DEP as well. In principle, it was shown that enzymes are active after immobilization by DEP, but no quantification of the retained activity was reported so far. In this study, the activity of the enzyme horseradish peroxidase (HRP) is quantified after immobilization by DEP. For this, HRP is immobilized on regular arrays of titanium nitride ring electrodes of 500 nm diameter and 20 nm widths. The activity of HRP on the electrode chip is measured with a limit of detection of 60 fg HRP by observing the enzymatic turnover of Amplex Red and H<sub>2</sub>O<sub>2</sub> to fluorescent resorufin by fluorescence microscopy. The initial activity of the permanently immobilized HRP equals up to 45% of the activity that can be expected for an ideal monolayer of HRP molecules on all electrodes of the array. Localization of the immobilize on the electrodes is accomplished by staining with the fluorescent product of the enzyme reaction. The high residual activity of enzymes after AC field induced immobilization shows the method's suitability for biosensing and research applications.

## KEYWORDS

AC electrokinetics, dielectrophoresis, enzyme activity, immobilization, nanoelectrodes

## 1 | INTRODUCTION

Dielectrophoresis (DEP) is the force acting on a polarizable particle in a nonuniform electric field [1]. The frequency-dependent Clausius–Mossotti factor  $K(\omega)$ , and therefore the frequency-dependent permittivity of particle

and medium, defines whether a particle experiences attraction (positive DEP) or repulsion (negative DEP) in high electric field gradients [2].

$$F_{\text{DEP}} = 2\pi r_p^3 \epsilon_0 \epsilon_m \text{Re}[K(\omega)] \nabla |E|^2 \quad (1)$$

DEP is mainly applied to cells, which can be trapped, isolated, sorted, separated, or characterized by DEP [3]. As the force directly depends on the volume of the particle, the immobilization of smaller particles requires higher

**Abbreviations:** DEP, dielectrophoresis; HRP, horseradish peroxidase; ITO, indium tin oxide; LOD, limit of detection; NA, numerical aperture; PEG, polyethylene glycol; RPE, R-phycoerythrin; TiN, titanium nitride.

This is an open access article under the terms of the [Creative Commons Attribution](https://creativecommons.org/licenses/by/4.0/) License, which permits use, distribution and reproduction in any medium, provided the original work is properly cited.

© 2022 The Authors. Electrophoresis published by Wiley-VCH GmbH.

field gradients (see Equation 1), which can be produced by sharp electrode geometries. This way, submicron particles, for example, polystyrene beads and virus particles, can be separated or immobilized by DEP as well [4, 5]. Although the mechanism behind the phenomenon is still a subject of recent studies and discussions [6–10], proteins [11, 12], enzyme molecules [13], and even small dye molecules [14] were also manipulated by DEP. As the immobilization on nanoelectrodes is label free and accomplished in seconds [15, 16], DEP might become a method of choice for the production of biosensors. Furthermore, protein molecules can be immobilized as singles as has been shown with pairs of planar nano-electrode tips and R-phycoerythrin (RPE) [12]. In a first attempt to produce a protein nanoarray for single-molecule experiments, bovine serum albumin (BSA) was immobilized on a small nanoelectrode array of nine electrodes with a tip diameter of 30 nm. The protein molecules were immobilized either permanently or temporarily, dependent on the applied field strength, but were not proven to be isolated as singles yet [15]. For the immobilization of single enzymes or protein molecules on arrays, sharp electrode tips with a diameter below the particles diameter are required [16, 17]. Recent advances in the standard complementary metal-oxide-semiconductor production process of silicon-based electrode arrays by reactive ion etching allowed the standardized production of sufficiently small electrode tips: arrays of thousands of cone-shaped electrodes were produced with a minimal diameter of about 1.5 nm, which can be adjusted to larger diameters by chemical mechanical polishing [16].

For biosensors, lab-on-chip-devices and single enzyme molecule experiments, not only the reliable trapping, but also a high residual activity of the involved enzymes has to be ensured. In principle, the amount of immobilized BSA was estimated [18] and the activities of anti-RPE antibodies and horseradish peroxidase (HRP) were shown [13, 19]. However, there was no absolute quantification of the immobilize's activity. In order to evaluate the applicability of DEP-immobilized enzyme arrays, the present study provides a quantitative determination of the activity of enzyme molecules permanently immobilized merely by DEP.

As a model enzyme, HRP was chosen. HRP is a single subunit, 44 kDa heme protein with a known three-dimensional structure and catalytic pathway and a complex glycosylation pattern [20, 21]. This enzyme has been studied intensively for centuries and has become a standard chemical for diagnostic kits and immunoassays because of its availability, high stability, and high activity in colorimetric and fluorometric assays [22]. For similar reasons, it is a popular enzyme for the proof-of-principle for single enzyme molecule experiments [23–28] and was already shown to be active after DEP on nanoelec-

trode arrays [18]. In this study, we have employed titanium nitride (TiN) ring electrode arrays, which combine the advantages of the well-established tungsten cylinder electrode arrays [13, 17, 18] with a smaller electrode geometry of only 20 nm width.

## 2 | MATERIALS AND METHODS

### 2.1 | Materials

HRP (EC 1.11.1.7) Type VI-A was purchased from Sigma. BSA (Albumin Fraction V for western blotting, from bovine serum) was acquired from Applichem. Both were dissolved in deionized water to give a final concentration of 4 mg/ml. Protein concentrations were measured using each protein's molar extinction coefficient (HRP:  $\epsilon_{403\text{ nm}} = 102\text{ mM}^{-1}\text{ cm}^{-1}$ ; BSA:  $\epsilon_{280\text{ nm}} = 43.8\text{ mM}^{-1}\text{ cm}^{-1}$  [29, 30]) using a Nanodrop spectrophotometer ND-1000 (PEQLAB Biotechnologie GmbH). Stock solutions were stored at  $-20^{\circ}\text{C}$ . For spectroscopic activity measurements of free HRP, the enzyme was diluted using phosphate buffer with 0.1% BSA and 0.1% Triton X 100. Amplex Red (10-acetyl-3,7-dihydroxyphenoxazine) was purchased from Cayman Chemical, dissolved in dimethyl sulfoxide, and stored at  $-20^{\circ}\text{C}$ . Dilutions were prepared on the day of use in deionized water. 30%  $\text{H}_2\text{O}_2$  was purchased from Merck and also diluted daily. All dilutions were stored on ice and protected from light. Phosphate buffer pH 7.5 was prepared by mixing 100 mM  $\text{KH}_2\text{PO}_4$  (Roth) and 100 mM  $\text{K}_2\text{HPO}_4$  (Acros Organics) until the desired pH was reached. The buffer was filtered using 0.22  $\mu\text{m}$  syringe filters and stored at  $+7^{\circ}\text{C}$  or  $-20^{\circ}\text{C}$ . PEG 20,000 (polyethylene glycol,  $M \approx 20,000\text{ g/mol}$ ) was purchased from Roth and was dissolved in deionized water to a final concentration of 2% (w/v), filtered, and stored at  $-20^{\circ}\text{C}$ . Resorufin (Biotium) was dissolved in dimethylformamide resulting in a concentration of 1 mM and was diluted in phosphate buffer before use.

### 2.2 | Inactivation of HRP

HRP was inactivated following a published protocol with minor modifications [31]. HRP at a final concentration of 0.44 mg/ml was incubated for 2 h with 6 mM sodium azide and 6 mM  $\text{H}_2\text{O}_2$  in phosphate buffer. After inactivation, the buffer was changed against sodium bicarbonate buffer pH 8.7 in six cycles using an Amicon Ultra-4 centrifugal filter unit with a molecular cutoff of 30 kDa. In a 2.6  $\mu\text{M}$  Amplex Red assay using the fluorescence spectrometer, the activity of the inactivated HRP was determined to 0.06% of the

initial enzyme activity. The inactivated enzyme was stored at  $-20^{\circ}\text{C}$ . For DEP, an aliquot was thawed, and the buffer was exchanged against deionized water in 10 cycles using a VivaSpin 500 centrifugal concentrator with a molecular cutoff of 30 kDa. The final concentration of the inactivated enzyme was 2.2 mg/ml. The sample was stored at  $-20^{\circ}\text{C}$  in aliquots.

## 2.3 | Microscopy

Two upright fluorescence microscopes were used in this study: Olympus BX51 and Olympus BX53. Both microscopes were equipped with an LED illumination system (CoolLED pE4000; Acal BFi), a 60 $\times$  objective with a numerical aperture (NA) of 0.7 and a long working distance (LUCPlan FLN, Olympus) and a 100 $\times$  objective with NA = 0.9 for imaging in air (MPlanFL; Olympus), which were used for all measurements and fluorescence images shown here. Using the Olympus BX51, images were acquired using the Software Cell<sup>M</sup>, which controlled a cooled CCD camera (F-View II; SIS—Soft Imaging System/Olympus) and a shutter driver (Uniblitz Model VCM-D1; Vincent Associates, Rochester, NY). For Amplex Red assays on this microscope, the filter set WIG (U-MWIG3 from Olympus, with excitation filter BP 530–550, dichroic mirror 570 and emission filter BA575IF) was used. The Olympus BX53 was equipped with a sCMOS camera (Orca flash 4.0, Hamamatsu) and controlled using the manufacturer's software CellSens Dimensions, which allowed to control the light source with a virtual shutter. Amplex Red assays and fluorescence micrographs of resorufin-stained samples were monitored using the filter set Cy3 (Chroma UF39004 with excitation filter AT540/25x, dichroic mirror AT565DC, and emission filter AT605/55 m). Rhodamin 123 staining was imaged using the filter set FBW (Olympus U-FBW, emission 460–495 nm; dichroic mirror 505 nm, emission filter 510IF). Images were processed using ImageJ (<http://imagej.nih.gov/ij>) [32].

For scanning electron microscopy, the microscope Zeiss EVO MA 10 with the manufacturer's software SmartSEM (version 5.07) was used. An acceleration voltage of 3 kV was applied at a low beam current of 9 pA. The working distance was 5 mm. No preparation of the sample was necessary. The atomic force microscope (NanoWizard 3, JPK Instruments) was used with a cantilever with a spring constant of 42 N/m and a sharpened tetrahedral silicon tip (OMCL-AC160BN-A2, Olympus) in tapping mode. Imaging was performed in air and images were processed using Gwyddion, a free open-source software for scanning probe microscopy data visualization and analysis (<http://gwyddion.net>) [33].

## 2.4 | Amplex Red assays

For the measurement of HRP activity, Amplex Red and  $\text{H}_2\text{O}_2$  were used as substrates. A substrate solution with either 2.6  $\mu\text{M}$  or 26  $\mu\text{M}$  Amplex Red, 88  $\mu\text{M}$   $\text{H}_2\text{O}_2$ , and 0.1% (w/v) PEG 20,000 in phosphate buffer was prepared shortly before use. For the characterization of the enzyme, measurements were done with the luminescence spectrometer Perkin Elmer LS 55. Acrylic cuvettes with a path length of 10 mm (Sarstedt, REF 67.755) were used and filled with 1.5 ml substrate solution. The reaction was monitored for 60 s with  $\lambda_{\text{ex}} = 540$  nm and  $\lambda_{\text{em}} = 610$  nm. The turnover rates were calculated from the linear increase in fluorescence intensity using a calibration curve, which was determined with resorufin standards.

For on-chip Amplex Red assays, the substrate solution was prepared in a reaction tube and protected from light until use. A small piece of a silicone foil with 100  $\mu\text{m}$  thickness (Wacker ELASTOSIL Film 2030 250/100) with a  $\varnothing 5$  mm hole was placed on a 12 $\times$ 12 mm cover glass #1. For bringing the electrode array into focus, 1.5  $\mu\text{l}$  phosphate buffer was pipetted onto the prepared cover glass, which was then placed onto the chip. The luminous-field diaphragm was partly closed to avoid unnecessary photobleaching or photooxidation. After focusing, cover glass and chip were separated, cleaned with deionized water, and dried using an  $\text{N}_2$  stream. Then, the substrate solution was placed between cover glass and chip in the same way as the buffer. The chip was carefully placed under the 60 $\times$  objective and a measurement was started. By this procedure, manual focusing with the substrate solution in place was avoided to minimize photooxidation. The increase in fluorescence was observed using the Cy3 (Olympus BX53) or WIG (Olympus BX 51) filter set and the 550 nm LED at 100% output. Images were taken in 10 s intervals for 2 min using the automated image acquisition and an automated shutter. The exposure time was 200 ms (Olympus BX51) or, because of the higher sensitivity of the used sCMOS camera, 50 ms (Olympus BX53). After the fluorescence image acquisition, a brightfield image was taken to check the positioning of the electrodes in the focal plane. If necessary, the positioning was corrected for the next measurement. Turnover rates were calculated from the increase in brightness in a fixed region of interest in the acquired image stack. Calibration curves for resorufin fluorescence, which were acquired for each of the microscopes, were applied. The HRP concentration and mass was calculated from the turnover rate using calibrations, which were measured at the luminescence spectrometer. For convenience, an ImageJ macro was written that streamlined image analysis. Exponential fits were calculated

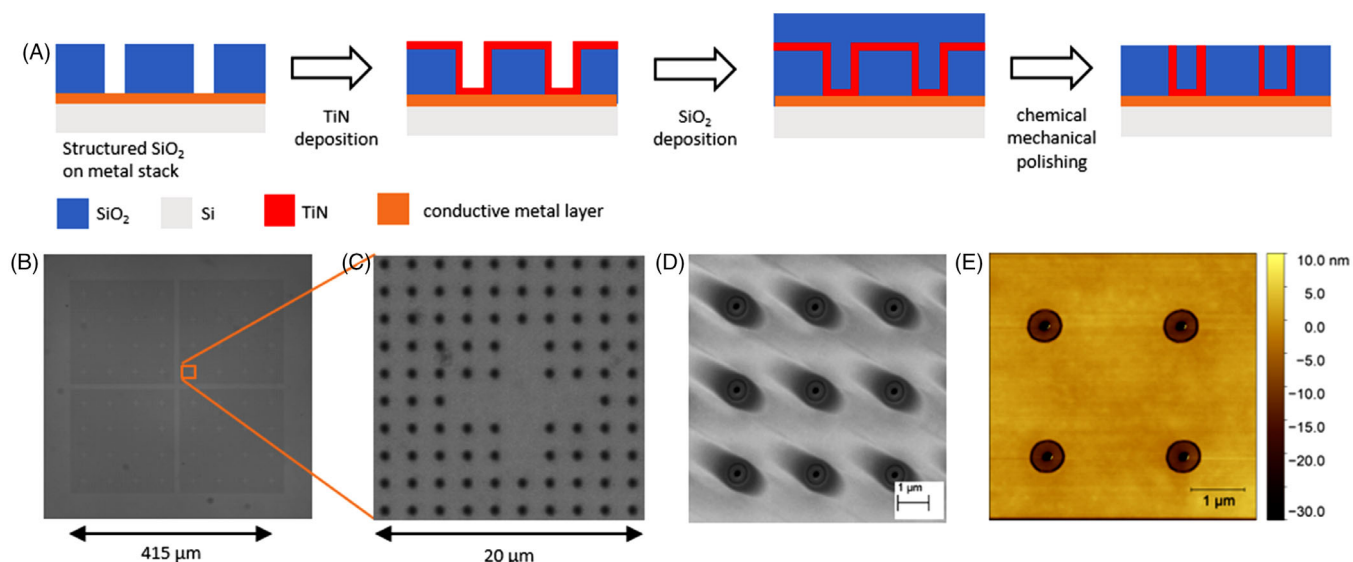


**FIGURE 1** Titanium nitride (TiN) ring electrode arrays. (A) Scheme of the production process for TiN ring electrode arrays. (B) Brightfield image of the complete array, consisting of four subarrays (20×). (C) Section of the same array, containing an orientation cross without electrodes (100×). (D) Scanning electron microscope image. (E) Atomic force microscope image

using OriginPro 2019 based on a Levenberg–Marquardt algorithm.

## 2.5 | Electrode arrays

Electrode chips were produced in a standard 0.25 μm complementary metal-oxide-semiconductor protocol on 8 inch silicon wafers. Each array consisted of four subarrays containing 6256 electrodes. For easier orientation on a chip, some electrodes were omitted leaving cross-shaped areas. Tungsten cylinder electrodes had a diameter of about 500 nm and a gap of about 2 μm. The cylinders were embedded in SiO<sub>2</sub>. All electrodes of a subarray were electrically connected by an underlying conducting metal layer [13]. For details on the production process, please refer to Otto et al. [19]. TiN ring electrodes were produced using the same layout as the current batch of tungsten cylinder electrodes (Figure 1B, C) [12]. As for tungsten cylinders, a SiO<sub>2</sub> layer was deposited on a metal stack and structured by etching cylindrical holes into it. The holes were lined with a 20 nm TiN layer and filled with SiO<sub>2</sub> by chemical vapor deposition. Excess SiO<sub>2</sub> and TiN on the surface were removed by chemical mechanical polishing (Figure 1A). Scanning electron and atomic force microscope images show that the rings are not filled completely (Figure 1D, E). In the case of TiN ring electrodes, all four subarrays on a chip are electrically connected to each other and are set on the same potential.

## 2.6 | Dielectrophoresis

For DEP, a cover glass with a conductive layer of indium tin oxide (ITO, SPI Supplies, 70–100 Ω) was used as a counter electrode. Electrode chips were mounted to microscope slides and connected to a socket for the application of electric fields. Consecutive numbers were assigned to the mounted chips. Electrical connections to the indium tin oxide surface and to the contacting patches of the electrode chips were prepared by using a carbon-based conductive glue (Leit-C, Plano). A commercially available silicone film with a thickness of 100 μm (Wacker ELASTOSIL Film 2030 250/100) was cut into squares with a ø4 mm hole and used as spacer material between ITO and chip. A protein sample dissolved in deionized water was placed between electrode chip and ITO counter electrode (Figure 2A). The conductivities of the samples amounted to about 45 μS/cm for HRP, below 45 μS/cm for inactivated HRP, and 75 μS/cm for BSA.

Alternating currents were generated using a function generator (Wavetek model 193) and a wide band amplifier (Toellner TOE 7606). Frequency and amplitude of the signal were monitored using a counter (Voltcraft 7202), oscilloscope (Rhode & Schwarz RTC1002), and RMS voltmeter (Rhode & Schwarz URE) (Figure 2B). For the immobilization of proteins, a frequency of 10 kHz and an amplitude of 7 V<sub>RMS</sub> (20 V<sub>pp</sub>) were set and applied to the electrode chip for 10 min. After DEP, the chip was rinsed with deionized water and incubated three times for about



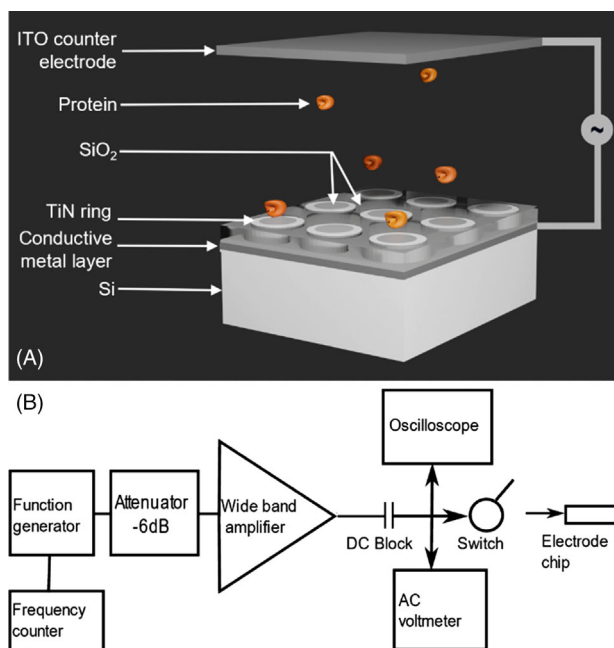


**FIGURE 2** Schemes of the experimental setup for dielectrophoresis (DEP) experiments. (A) Schematic three-dimensional view (not to scale). (B) Electrical setup

5 min under phosphate buffer. After each incubation step, it was again rinsed with deionized water.

## 2.7 | Cleaning and reuse of chips

Tungsten cylinder electrode chips were cleaned by extensive rinsing using deionized water and by the application of the First Contact cleaning polymer (Photonic Cleaning Technologies). Before use, the chips were exposed to an  $N_2$  plasma for 10 min using the KinPen (Neoplas). TiN ring electrodes are chemically more inert than tungsten and were cleaned using deionized water, First Contact cleaning polymer and peroxymonosulfuric acid (“piranha solution”). Piranha solution was prepared directly on-chip by mixing 4  $\mu$ l  $H_2SO_4$  (96%) with 1.2  $\mu$ l  $H_2O_2$  (30%). After 5 min of incubation, the chip was rinsed with deionized water, shortly incubated with 1.25 M NaOH and washed in diluted phosphate buffer for 15 min.

## 3 | RESULTS

### 3.1 | Activity of HRP in solution

HRP catalyzes the oxidation of the colorless substrate Amplex Red by  $H_2O_2$  to resorufin, which is highly fluorescent with an excitation maximum at 563 nm and an emission maximum at 587 nm [34]. In order to cal-

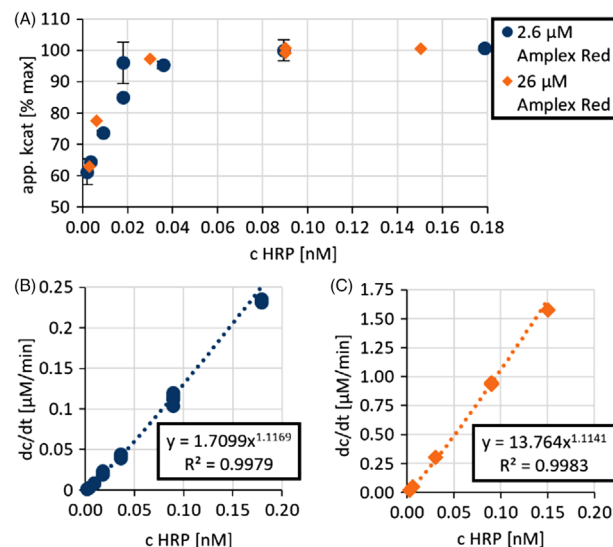


**FIGURE 3** Concentration dependent activity of horseradish peroxidase (HRP) toward Amplex Red and  $H_2O_2$ . (A) Apparent  $k_{cat}$  for both tested Amplex Red concentrations. (B and C) Nonlinear regression for the calculation of the HRP concentration from the increase in resorufin fluorescence. (B) 2.6  $\mu$ M Amplex Red. (C) 26  $\mu$ M Amplex Red

culate the exact amount of HRP in a sample from the velocity of the turnover reaction, the HRP activity has to be known exactly. As already reported by Gorris and Walt, the apparent Amplex Red turnover rates are dependent on the HRP concentration [26]. This is probably the case because the final step in the building of resorufin is an enzyme-independent dismutation reaction of two Amplex Red radicals [35]. Those are more likely to react otherwise, that is, with surfaces, if the allover HRP and Amplex Red radical concentration is low [26]. Therefore, the concentration-dependent activity of HRP was measured for two Amplex Red concentrations (2.6  $\mu$ M and 26  $\mu$ M) using a fluorescence spectrometer (Figure 3A). For both assays, the HRP activity reached its maximum above a HRP concentration of 0.03 nM. For concentrations above 0.03 nM HRP, the turnover rate  $dc(\text{resorufin})/dt$  depends linearly on the HRP concentration. The apparent maximum turnover rates for Amplex Red to resorufin were  $21.6 \pm 0.7 \text{ s}^{-1}$  (2.6  $\mu$ M Amplex Red) and  $174 \pm 2 \text{ s}^{-1}$  (26  $\mu$ M Amplex Red). At the lowest measured concentrations, the apparent HRP activity was reduced to about 60%–65% of the maximum activity. The measurement range for the assays on the chip cannot be restricted to the concentration range above 0.03 nM, because an upper bound of 1.9 pg HRP is expected to be immobilized as a molecular layer on the TiN ring electrode arrays, resulting in a concentration of 0.03 nM in 1.5  $\mu$ l reaction volume. Therefore, nonlinear calibration curves were prepared (Figure 3B, C) for the calculation of the HRP concentration from an unknown

sample. The resulting equation is:

$$\text{HRP [nM]} = f \sqrt{\frac{1}{g} \cdot \frac{dc_{\text{Resorufin}}}{dt}} \quad (2)$$

For  $c(\text{Amplex Red}) = 26 \mu\text{M}$ :  $f = 1.12$ ;  $g = 1.76$

For  $c(\text{Amplex Red}) = 2.6 \mu\text{M}$ :  $f = 1.14$ ;  $g = 13.76$

### 3.2 | On-chip measurements of HRP activity by fluorescence microscopy

For the determination of the HRP activity on an electrode chip, a measurement chamber containing  $1.5 \mu\text{l}$  of the Amplex Red substrate solution was built directly onto the chip's surface. The increase in resorufin concentration was monitored using a fluorescence microscope. To prove this measurement principle, known HRP concentrations were added to the substrate solution before placing it on a clean electrode chip, which resulted in pg amounts of HRP in the measurement chamber. Furthermore, blank measurements with the Amplex Red substrate solution, but without any HRP, were performed. For the calculation of the amount of HRP on the chip or in the sample volume, respectively, the fluorescence in a region of interest was measured in 10 s intervals. The velocity of the turnover of Amplex Red to resorufin in the first minute of observation was calculated using calibration curves for the resorufin fluorescence, which were measured under the same experimental conditions (Figure 4A). The amount of HRP which this turnover rate could be assigned to was then calculated using Equation (2). These experiments were performed with two Amplex Red concentrations to test which concentration is more advantageous for measuring HRP concentrations on the chip. For  $26 \mu\text{M}$  Amplex Red, a higher HRP activity and therefore higher sensitivity was expected, but also stronger effects of product accumulation or adsorption to surfaces and by photooxidation.

On freshly cleaned TiN ring electrode chips, the background activity without any HRP was found to amount to only  $0.005 \pm 0.001 \text{ pg HRP}$  in assays with  $26 \mu\text{M}$  Amplex Red. When free HRP was added to the on-chip Amplex Red assay, a linear increase in resorufin fluorescence with time was measured (Figure 4B) and the HRP activity was quantified. Two HRP concentrations were tested to determine the accuracy and reproducibility of the assays. The assay containing  $26 \mu\text{M}$  Amplex Red had a tendency to overestimate the amount of HRP (Figure 4C), but also had a smaller standard deviation for low HRP amounts and a lower background noise. The limit of detection (LOD) of both assays was calculated using Equation (3) [36]. This results in a LOD of  $0.06 \text{ pg HRP}$  for the assay with  $26 \mu\text{M}$  Amplex Red and  $0.12 \text{ pg}$  for the assay with  $2.6 \mu\text{M}$  Amplex

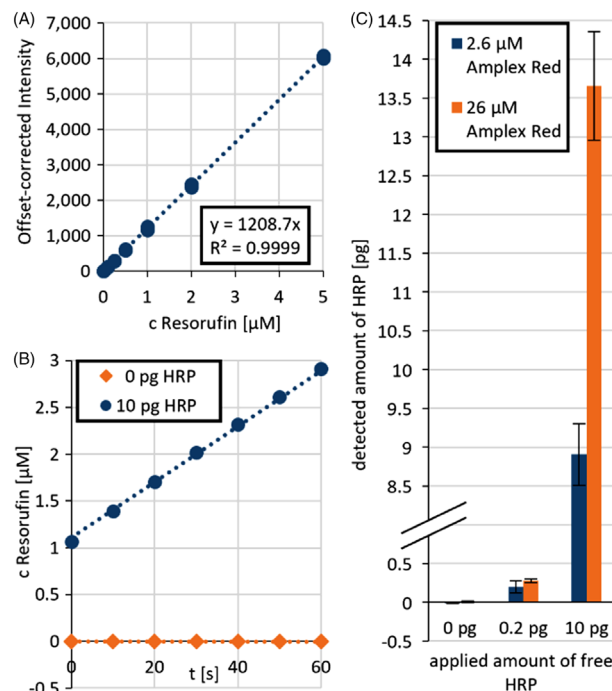


**FIGURE 4** On-chip Amplex Red assay with free horseradish peroxidase (HRP) on titanium nitride (TiN) ring electrodes. (A) Calibration curve for the measurement of resorufin concentrations using the microscope Olympus BX53. (B) Example of increase in resorufin fluorescence in the  $26 \mu\text{M}$  Amplex Red assay with 10 pg free HRP and with a blank sample without HRP. (C) Results for the measured amount of free HRP in samples with known HRP concentration on-chip using two different Amplex Red concentrations

Red. As rather small amounts of HRP are expected on the chip after DEP, the assay containing  $26 \mu\text{M}$  Amplex Red was chosen for further measurements. For comparison, the LOD of the method using the fluorescence spectrometer was calculated, too, giving a value of  $13.3 \text{ pg HRP}$ . The standard deviations of the cuvette-based spectrometer data were a tenth of the microscope data, resulting in a lower LOD for HRP if concentrations are considered. However, the LOD for the absolute amount of enzymes is 100 times higher because of the 1000-fold larger volume of the cuvette.

$$\text{LOD} = \bar{y}_{\text{blank}} + 1.645 \cdot \sigma_{\text{blank}} + 1.645 \cdot \sigma_{\text{low}} \quad (3)$$

where  $\bar{y}_{\text{blank}}$  = mean of blank measurements;  $\sigma_{\text{blank}}$  = standard deviation of flank measurements; and  $\sigma_{\text{low}}$  = standard deviation of the lowest tested concentration.

When tungsten cylinder electrodes were used for the experiments, background activities without HRP were very high. The velocity of the turnover equaled an amount of up to 3 pg of free HRP on the electrode chip. Therefore,

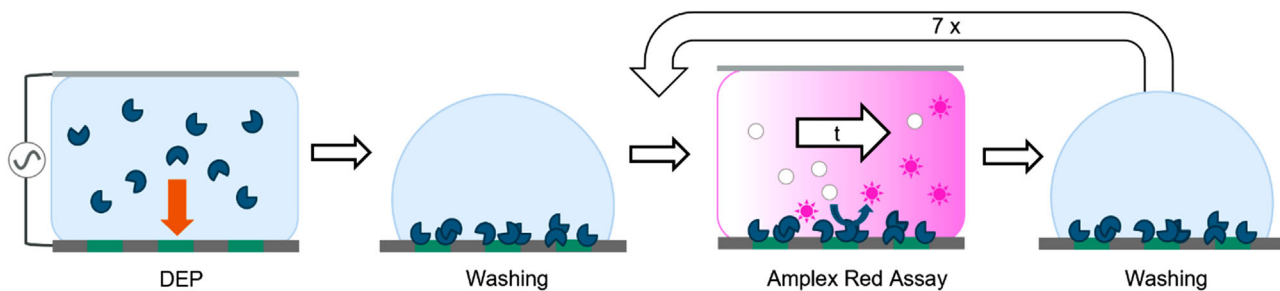


FIGURE 5 Scheme of the experimental procedure of horseradish peroxidase (HRP) immobilization and activity measurements on titanium nitride (TiN) ring electrodes

tungsten cylinder electrodes were not used in experiments with HRP.

### 3.3 | HRP on TiN ring electrodes: Immobilization and activity measurements

HRP was immobilized on TiN ring electrodes by DEP. A voltage of  $7 V_{RMS}$  and a frequency of 10 kHz were applied for 10 min. Very similar experimental conditions were shown to be suitable to immobilize both HRP and BSA on tungsten cylinder electrodes [13, 18]. For immobilization of unlabeled HRP, 4 mg/ml of the enzyme dissolved in deionized water was incubated on the electrode chip 01. The electrode chip with immobilized HRP was washed three times with phosphate buffer. Afterward, the HRP activity on the chip was measured seven times with Amplex Red assays (26  $\mu$ M Amplex Red) followed by washing of the chip after each measurement (Figure 5). The initial activity on the chip equaled 7.5 pg of free HRP and appeared to incline asymptotically toward a finite value. Therefore, least-squares fits were performed to gain more information from the collected data set. Three models were considered and tested to show which one represented the data best. Equation (4) describes simple washing off of adsorbed HRP from the chip surface according to Nernst's distribution law. Equation (5) includes a constant term which would represent a permanently immobilized fraction of HRP. In Equation (6), a possible, linear inactivation or desorption of the permanently immobilized HRP fraction is considered. Using these models, exponential fits were performed on the obtained data (Figure 6).

$$m_{HRP} [pg] = m_1 \cdot e^{-\frac{N}{k_1}} \quad (4)$$

$$m_{HRP} [pg] = m_1 \cdot e^{-\frac{N}{k_1}} + m_2 \quad (5)$$

$$m_{HRP} [pg] = m_1 \cdot e^{-\frac{N}{k_1}} + m_2 + m_3 N \quad (6)$$

with  $N$  = number of measurement and washing cycles;  $m_1$  = temporarily adsorbed HRP;  $k_1$  = washing rate of  $m_1$ ;  $m_2$  = permanently immobilized HRP;  $m_3$  = inactivation desorption rate of  $m_2$ .

The best fit was achieved using the model described by Equation (6). The fitted curve aligned with the data almost perfectly and showed the highest corrected  $R^2$ . As compared to a simple  $R^2$  value the corrected  $R^2$  takes into account the number of free parameters and allows a better comparison between models differing in complexity. The introduction of the additional parameter  $m_3$  also removed an increasing trend in the residual plot (Figure 6).

The immobilization by DEP, washing with phosphate buffer, and a sequence of Amplex Red assays (Figure 5) were repeated on the same chip after piranha-cleaning. Three other chips with TiN ring electrodes were used for two runs of this experiment as well. In some cases, the number of measurements after immobilization and washing was increased to up to 14 for a more significant result. For most of the runs, the fit following Equation (6) again described the obtained data best. The second run of the experiment on chip 01 resulted in similar parameters as the first one, but with higher uncertainties of the parameters (Figure 7). Measurements on chip 03 showed a similar behavior as HRP on chip 01 in both experiments (Figure 7). The data with the best fitted curve for each experiment and the residual plot are shown in Table S1.

The experiments on electrode chips 02 and 04 resulted in less successful HRP immobilization. In one experiment, on each of these chips very small activities of the immobilized HRP were detected. The data did not allow to calculate the parameter  $m_3$  reasonably. Instead, the simpler model represented by Equation (5) resulted in the best fit. Affected fit parameters are marked with "a" in Figure 7 or were not detectable (n.d.) at all. If permanently immobilized HRP was detectable on these chips, the measured amount was up to 10 times lower than on chip 01 and chip 03 (Figure 7). The data and best fits for chip 02 and 04 are shown in Table S1.

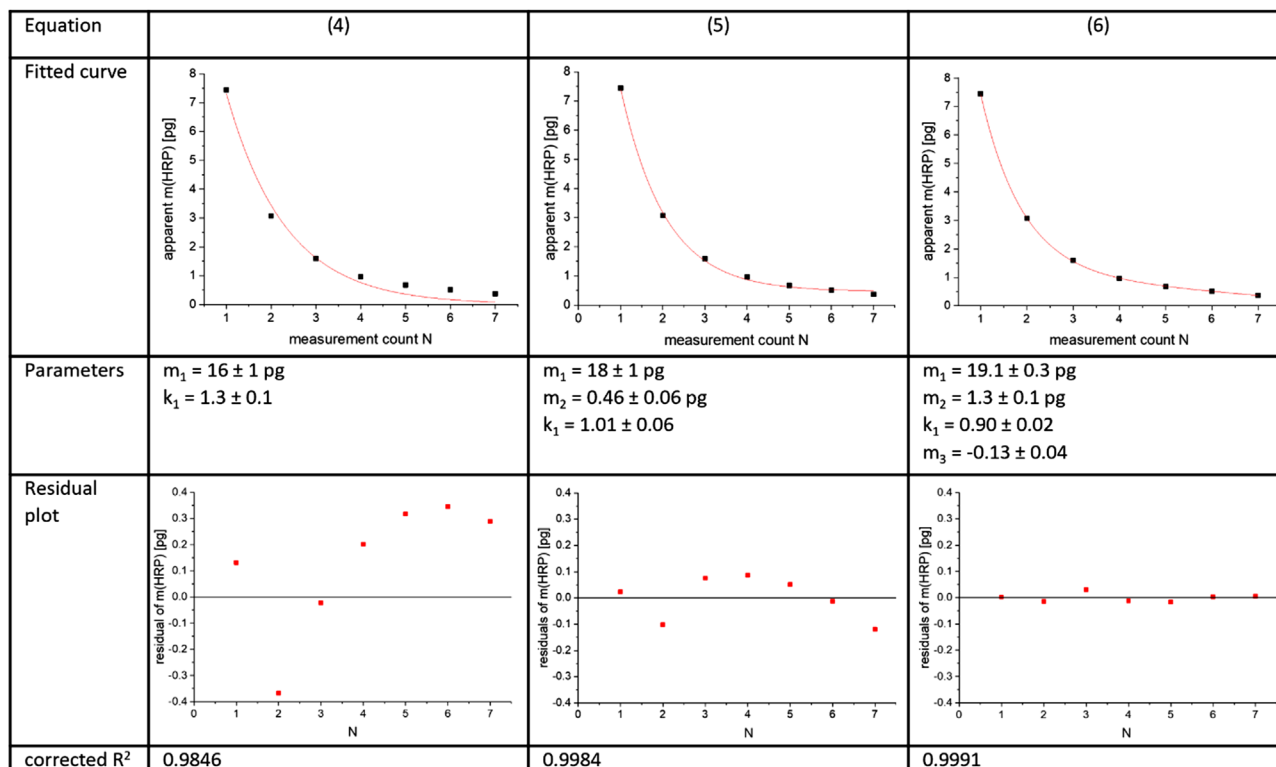


FIGURE 6 Results of exponential fits for the description of the increase of horseradish peroxidase (HRP) activity after dielectrophoresis (DEP) on chip 01, run 1

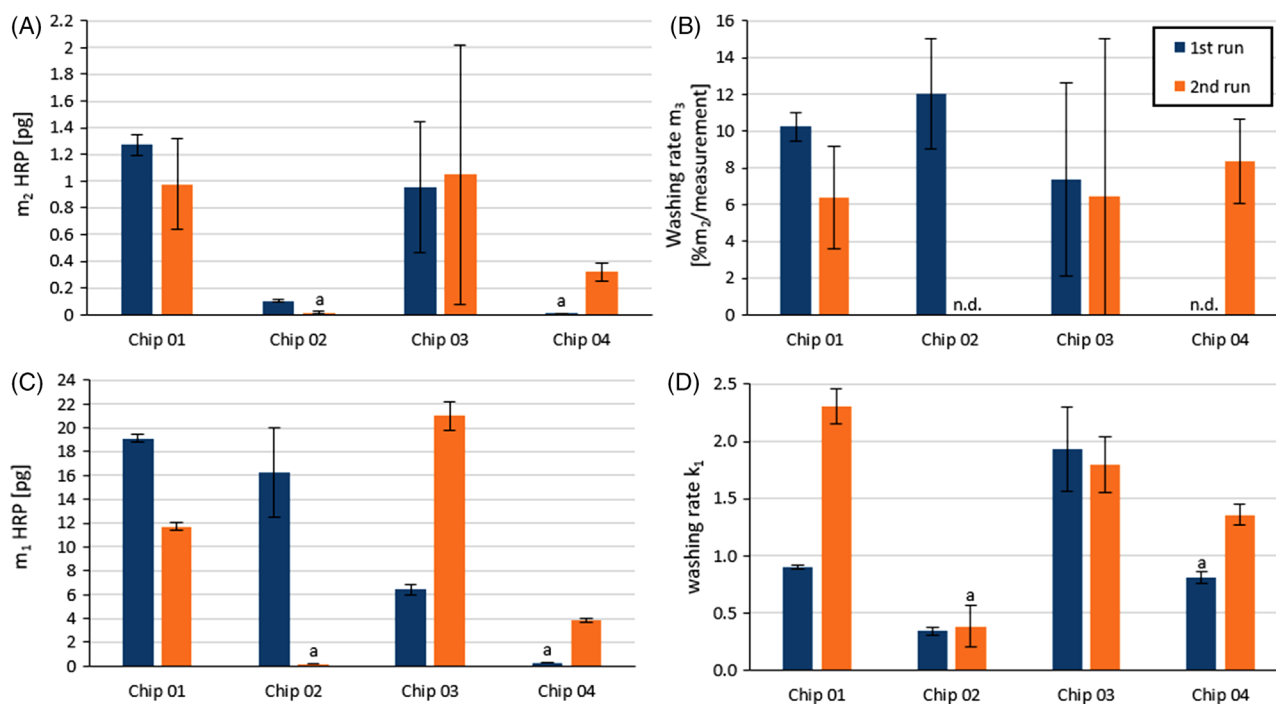
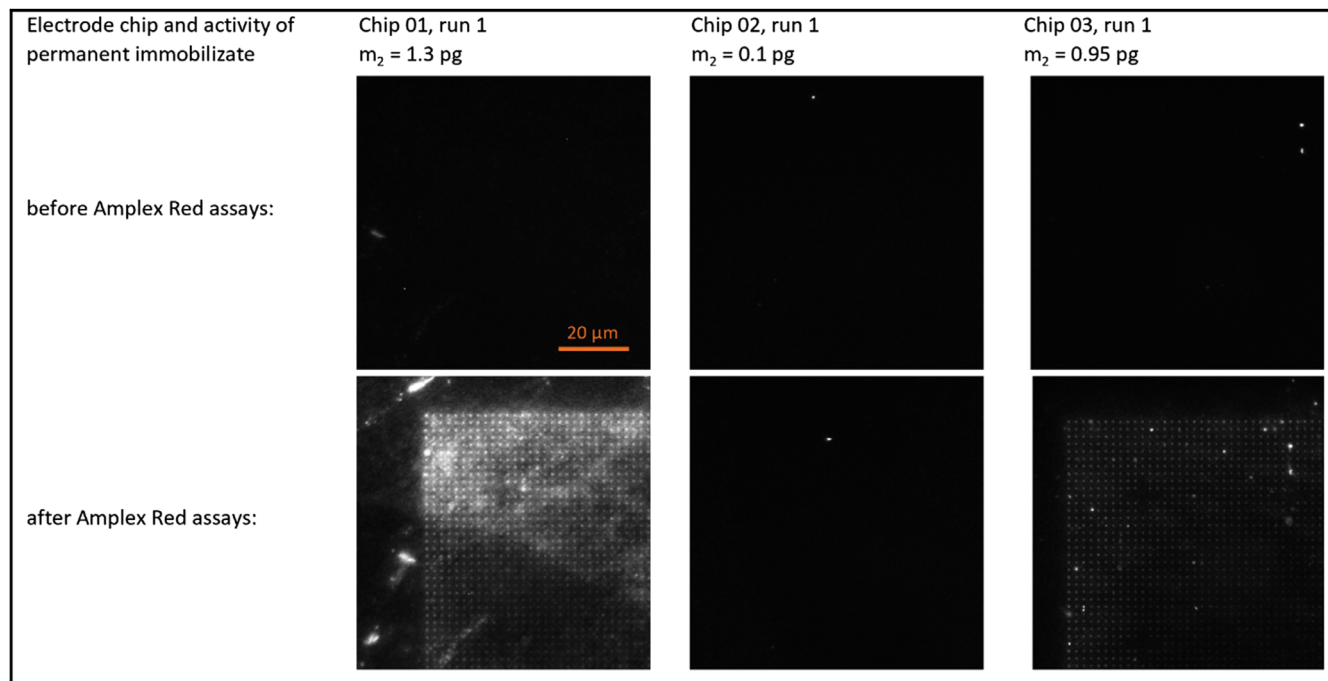


FIGURE 7 Activity of permanently immobilized horseradish peroxidase (HRP) on titanium nitride (TiN) ring electrode chips. HRP was immobilized by dielectrophoresis (DEP), washed, and characterized by Amplex Red assays (26  $\mu$ M Amplex Red) two times on each chip. For further analysis, the obtained data was fitted using model Equation (6) or, in cases indicated with a, Equation (5). Error bars show the standard deviation of the parameter given by the fit program. (A) HRP activity of the permanently immobilized enzyme fraction ( $m_2$ ). (B) Washing rate  $m_3$  thereof (n.d.: not detected). (C) HRP activity of the temporarily adsorbed enzyme fraction ( $m_1$ ). (D) Washing rate thereof ( $k_1$ )





**FIGURE 8** Fluorescence micrographs of a region of the titanium nitride (TiN) ring electrode array with immobilized horseradish peroxidase (HRP) before and after incubation with 26  $\mu\text{M}$  Amplex Red assays. Images were taken in air with the microscope Olympus BX53, objective 100 $\times$  NA = 0.9; Filter Cy3; LED 550 nm (100%) and an exposure time of 2 s. All images are shown with the same scaling and contrast settings

### 3.4 | Localization of active HRP immobilizes

Before and after the sequence of Amplex Red assays, fluorescence images of the electrode arrays were recorded. This allowed to detect residual resorufin sticking to the HRP immobilize. Resorufin fluorescence on the electrodes only increased when the permanently immobilized fraction  $m_2$  equaled 0.32 pg of free HRP or more. Resorufin was detected mainly on the electrodes. The fluorescence intensity was higher on the edges of the arrays, which is best seen on chip 03 (Figure 8). Even clearer evidence for the location of HRP on the chip would be possible if fluorescently labeled enzymes were used. Therefore, HRP samples were used for DEP after labeling the enzyme with either Cy5-NHS (Cytiva) or DY649P1-NHS (Dyomics) according to the manufacturer's protocol. However, the chosen enzyme label and purification method appear to have influenced the fluorescence of the immobilize and, more importantly, resulted in inactive immobilizes in most cases. This was not expected because labeling of the enzymes reduced their catalytic activity only slightly when assessed for freely diffusing HRP in solution.

### 3.5 | Control measurement 1: Incubation of HRP on chip without applied field prior to Amplex Red assay

To make sure that the active HRP was immobilized by DEP and not by random adsorption of the enzyme to the chip, blank measurements were performed. For that purpose, 4 mg/ml HRP was incubated for 10 min on a freshly cleaned chip, but no electric field was applied. After washing with phosphate buffer, series of six to seven Amplex Red assays (26  $\mu\text{M}$  Amplex Red) were performed. This experiment was carried out four times. Some HRP adsorbed temporarily to the chips, but it was washed off quickly in an exponential manner. The activity ceased to zero following model Equation (4) or, in one case, to a constant amount equivalent to 0.01 pg free HRP. The data together with the best resulting fit are shown in Table S2.

The activity of temporarily adsorbed HRP without an applied field was similar for the first experiments on chip 02 and chip 04, equaling 0.8–0.9 pg free HRP (Table 1). The second run on chip 02 and the one on chip 03 resulted in lower apparent HRP activities, equaling 0.4–0.5 pg. Therefore, the activities of temporarily adsorbed HRP molecules are an order of magnitude smaller than

**TABLE 1** Activity of horseradish peroxidase (HRP) on titanium nitride (TiN) ring electrode chips after incubation without applied field. HRP incubated on the chip, washed, and characterized by Amplex Red assays (26  $\mu$ M Amplex Red) in the same way as in experiments with applied field

Chip	run	$m_1$ [pg]	$m_2$ [pg]
02	1	$0.82 \pm 0.09$	n.d.
02	2	$0.43 \pm 0.04$	n.d.
03	1	$0.51 \pm 0.03$	n.d.
04	1	$0.87 \pm 0.06^a$	$0.011 \pm 0.009^a$

Note: For further analysis, the obtained data were fitted using model Equations (4)–(6). The result of the best fit is shown, which was obtained with Equation (4) or, in cases indicated with <sup>a</sup>; Equation (5).

Abbreviations: n.d.: no defined.

that for DEP experiments, which resulted in calculated activities of temporarily adsorbed enzymes of up to 21 pg free HRP (Figure 7).

After the experiments, the electrodes were checked for the adsorption of resorufin to the surfaces as shown in Figure 8. No additional resorufin fluorescence was detected on the chips.

### 3.6 | Control measurements 2: DEP with inactive proteins and Amplex Red assay on such immobilizates

The experiments with randomly adsorbed HRP showed that the apparent HRP activity on the chip is an effect of the applied electric field as it does not occur without an applied field. To check whether the increase in fluorescence intensity is caused by enzymatic turnover of Amplex Red and not by adsorption of trace amounts of resorufin to the immobilizate, surface protein samples without catalytic activity were immobilized and used in the same Amplex Red assay. For the first test, inactivated HRP was used. The enzyme was irreversibly inactivated by incubation with excess amounts of  $H_2O_2$  and sodium azide, which leads to the destruction of the heme center [31]. As a second sample, BSA was used. BSA was shown to be immobilized at similar DEP conditions on different nano-electrode arrays and showed no HRP-like activity [16, 18]. Both samples were immobilized successively on the freshly cleaned chip 01, which showed the best results after DEP with HRP before. After DEP and washing with phosphate buffer, each immobilizate was tested for HRP activity in a single Amplex Red assay. The activity on the chip equaled 0.006 pg for immobilized inactivated HRP and 0.004 pg for immobilized BSA. Both values correspond well with blank measurements on freshly cleaned chips. Furthermore, the immobilizates were checked for adsorbed resorufin by fluorescence microscopy in air. No additional resorufin fluorescence was found in comparison to images taken before

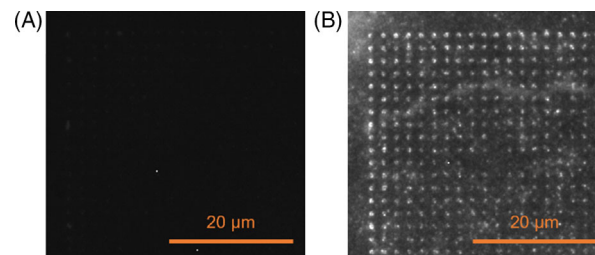


**FIGURE 9** Fluorescence micrographs of bovine serum albumin (BSA) immobilizate before (A) and after (B) incubation with 10  $\mu$ M rhodamine 123 in phosphate buffer for 5 min. Images were taken in air with the microscope Olympus BX53, objective 100 $\times$  NA = 0.9; Filter FBW; LED 470 nm (100%) and an exposure time of 2 s. Both images are shown with the same contrast settings

Amplex Red assays. This result was expected because the assay without any HRP involved contains only trace amounts of resorufin. Therefore, the chip was incubated with 2  $\mu$ M resorufin for 5 min. The immobilizates again showed no additional fluorescence. To show that protein molecules were really immobilized, the BSA immobilizate was also incubated with 10  $\mu$ M rhodamine 123 in phosphate buffer. Rhodamine 123 was already shown to strongly adsorb to protein surfaces immobilized by DEP [13] and acted accordingly in previous experiments with labeled BSA. Indeed, rhodamine fluorescence clearly increased at the electrode positions (Figure 9), proving that BSA was immobilized on the TiN ring electrodes. Even the circular shape of the electrodes was reproduced.

## 4 | DISCUSSION

### 4.1 | Evaluation of Amplex Red assays for the measurement of HRP activity on electrode chips

HRP activities were measured using Amplex Red assays. After characterizing the reaction kinetics using a fluorescence spectrometer, the assays were repeated in the smaller volumes on the chip and measured using the fluorescence microscope. On TiN ring electrodes, background activities without HRP were sufficiently low and HRP concentrations could be measured with both tested Amplex Red concentrations. The assay with 26  $\mu$ M Amplex Red was chosen for further investigation because of its lower LOD. A disadvantage of the high Amplex Red concentration is that the assay tends to overestimate the HRP concentration on the chip (Figure 4). This is possibly the case because the accumulated resorufin causes photooxidation of the remaining Amplex Red [37]. This inaccuracy is taken into account when measurement results are discussed, but appeared acceptable given the very low sample volume and proximity of the optical focus to surfaces.

When tungsten cylinder electrodes were used, the background activity of the chip surface without HRP was in the same order of magnitude as expected for a subarray fully covered with HRP. The apparent HRP activity can be attributed to the tungsten or tungsten oxide surfaces. Tungsten oxide nanoparticles are reported to catalyze redox reactions and photocatalytic oxidations [38, 39]. Other metal oxide nanoparticles also interfere with the Amplex Red assay [40]. Therefore, the tungsten cylinder electrode arrays are not suitable for the immobilization of HRP if the enzyme activity has to be measured with an Amplex Red assay. The tungsten electrodes may interfere with other assays for oxidoreductases as well.

## 4.2 | Activity of HRP on TiN ring electrodes after immobilization by DEP

On chip 01 and chip 03, all DEP experiments with active HRP led to successful immobilization of active protein. The best model for fitting the obtained HRP activity curves was represented by Equation (6) (Figure 6). For the first experiment on chip 01, the fit resulted in Equation (7), which can be interpreted as two different fractions of HRP immobilized on the chip.

$$m_{\text{HRP}} [\text{pg}] = 19.1 \text{ pg} \cdot e^{-\frac{N}{0.90}} + 1.3 \text{ pg} - 0.13 \text{ pg} \cdot N \quad (7)$$

$m_1$  represents the activity of only loosely bound HRP on the chip which is washed off in an exponential manner during the measurements. It equaled 19.1 pg of free HRP. A smaller fraction,  $m_2$ , represents HRP permanently immobilized by DEP. On chip 01,  $m_2$  shows as much HRP activity as is expected for 1.3 pg of free HRP in solution. As indicated by  $m_3$ , it is also washed off or inactivated, but only in a linear way. About 10% of the initial activity  $m_2$  is lost in each measurement cycle. For the second experiment on chip 01 and for both experiments on chip 03, Equation (6) again resulted in a satisfactory fit. The values for the parameters  $m_2$  (0.95–1.05 pg HRP) and  $m_3$  (6–7% of  $m_2$ ) were also similar (Figure 7). Fitting according to Equation (6) was still the best of the tested options, although it led to a rather high uncertainty in the fit parameters (Figure 7), higher residuals and a slightly lower corrected  $R^2$  than for the first experiment on chip 01 (Table S1), pointing to a further mechanism. Possibly residual enzyme fragments that stay on the chip after cleaning influence immobilization and washing of the freshly applied HRP. An additional variation of apparent fluorescence intensity might be caused by drift of the sample in z-direction resulting in some defocusing.

The determined amount of active HRP on chip 01 and 03 appears quite realistic, considering the geometry of the electrode rings and the size of the enzyme. On each chip, there are 25,024 electrode rings with an outer

radius of 500 nm and a width of 20 nm. This results in a total electrode surface of  $7.36 \times 10^{-10} \text{ m}^2$ . The radius of gyration of the enzyme is  $r_{\text{HRP}} = 2.65 \text{ nm}$  [41]. When the HRP molecules are packed densely on the surface, each molecule would occupy an area of  $2.8 \times 10^{-17} \text{ m}^2$ . Accordingly, about 1000 HRP molecules would fit on each electrode and  $4.4 \times 10^{-17} \text{ mol}$  enzyme molecules would fit onto the surfaces of all electrodes on a chip, which equates to 1.9 pg HRP. Taking into account that the Amplex Red assay with 26  $\mu\text{M}$  Amplex Red may overestimate the HRP activity on the chip (see Figure 4), the activity of the permanent enzyme immobilizes corresponds to 0.65–0.85 pg free HRP. This equals 34%–45% of the activity of those HRP molecules that would fit onto an enzyme monolayer on top of the electrode surfaces. An apparently reduced enzyme activity was expected for the HRP immobilize on electrode surfaces as compared to freely diffusing enzyme molecules. Reduced enzyme activities and diffusion limitations are drawbacks of many immobilization techniques [42]. Intrinsic effects of the surface of the solid support, for example, organized water layers as well as gradients of pH and of substrate concentration can affect the conformation, stability, and activity of enzymes and the observed turnover rates [43]. The orientation of the enzyme molecules relative to the surface also influences the activity. For  $\beta$ -galactosidase from *Lactococcus lactis*, the activity of the enzyme immobilized covalently on beads equals the activity of the free enzyme when the active site is oriented toward the solution, but reduced to one-third of its initial value when physically adsorbed to the surface in a random orientation [44]. When the active site of  $\beta$ -galactosidase from *Clostridium cellulovorans* is oriented in an angle of  $90^\circ$  to the surface normal, the activity is only 53% of the enzymes activity in solution [45]. With 34%–45% retained activity, the HRP immobilized on chip 01 and 03 was preserved to a similar degree as randomly oriented  $\beta$ -galactosidase. This allows to presume that HRP is also oriented randomly relative to the electrode surface and has not been inactivated by the electric field during immobilization. A further loss in activity can be expected due to the possibly unfavorable packing or stacking of enzyme molecules [43], but this apparently is not the case for HRP on TiN ring electrodes. Possibly the structure of the electrodes is small enough to create a distribution that allows a nearly undisturbed enzyme activity.

In all cases of successful immobilization of HRP on TiN ring electrodes, activity of the permanently immobilized enzyme fraction decreases by 6%–12% in the course of each experiment round (Figure 7B). This loss in activity might be due to inactivation or leaching of the enzyme molecules. A more careful handling of the chip, for example, by less intense rinsing between measurements or by avoiding the surface-active PEG supplement in the substrate solution, might reduce leaching of the immobilized HRP. Inactiva-

tion of HRP by excess  $\text{H}_2\text{O}_2$  is also possible, but typically occurs when  $\text{H}_2\text{O}_2$  is offered in excess without a reducing substrate [46, 47]. The applied excess in  $\text{H}_2\text{O}_2$  was only fourfold, which is reported to be optimal for the turnover of Amplex Red by free HRP [26].

In contrast to the results on chip 01 and 03, very low amounts of HRP were permanently immobilized on chip 02 and 04 (Figure 7). Apparently, there is some variation in the quality of the used TiN ring electrode chips, although they were direct neighbors on the same silicon wafer. Consequently, the immobilization of active HRP by DEP worked properly only on 50% of the tested chips, namely chip 01 and chip 03. The failure of the chips 02 and 04 may be a result of variations in the production process or in storage and handling of the chips, but still the main cause remains unclear.

### 4.3 | Localization of active HRP immobilizes

After measuring its HRP activity using Amplex Red assays and washing, the HRP immobilizes showed resorufin fluorescence (Figure 8). Apparently, the reaction product stuck to the enzyme surface. Fluorescence was higher at the edges of the arrays, indicating that the amount of immobilized HRP is also higher there. The same immobilization pattern is typically observed when immobilizing fluorescently labeled proteins on tungsten cylinder electrode arrays since the gradient of the electric field is higher at the edges of the array than in the center of the array [18].

Apparently, there is more than one monolayer of HRP immobilized at the edges of the array, but only the uppermost monolayer is assumed to be fully active. Lower enzyme layers will show reduced activity due to restricted substrate availability. The upper layer will restrict diffusion physically and deplete the local substrate concentration by its activity. Also, the edges of the array only represent a minor fraction of the electrodes. Therefore, the activity of the additional HRP layers on these electrodes can be neglected when the activity of the immobilize is discussed.

Labeling of the HRP before immobilization would have led to a clearer evidence for its location, but had to be omitted in this study. The enzyme label or residual free fluorophore molecules interfered with the immobilization of active enzyme molecules. The additional charges that are added to the enzyme by the fluorescent label possibly alter the effect of the electric field on the enzyme or reduce the stability of HRP at the surface. Since no modification of the enzyme is actually necessary for DEP itself and since the unlabeled enzyme gave more reliable results, the label-free method was preferred for this study.

### 4.4 | Control measurements

To rule out misinterpretation of the presented results, several control measurements were performed. In one approach, active HRP was incubated on the chips without an applied field. It resulted in no permanent immobilized HRP or a two orders of magnitude lower amount of permanently immobilized HRP as compared to experiments with successful DEP immobilization (Table 1). This shows that permanent immobilization of HRP in DEP experiments indeed is caused by the electric field and not by unspecific adsorption to the electrodes or to the silicon surface. The amount of temporarily adsorbed HRP was also clearly smaller than after successful DEP immobilization. Random adsorption can be higher in DEP experiments because the electric field also causes streaming effects [48]. The streaming HRP solution supplies more HRP molecules from the volume which can adsorb to surfaces than the stationary solution that can be depleted in enzyme molecules near the surface over time. Furthermore, the permanently immobilized HRP layer may adsorb additional enzyme molecules temporarily.

In a second approach, inactive proteins were immobilized by DEP and examined for possible apparent HRP activities. Neither the immobilize of inactivated HRP nor the BSA immobilize showed detectable HRP activity. It can be concluded that the increase in resorufin fluorescence in on-chip Amplex Red assays is caused solely by immobilized active HRP molecules, not by immobilized inactive proteins by, for example, adsorption of trace amounts of resorufin. The experiment also allowed some conclusions on the staining of the HRP immobilizes by resorufin, which was used to localize the active immobilize. No staining of the inactive proteins was observed after incubation with Amplex Red assays or with a resorufin standard. This indicates that the resorufin that accumulated in solution over time can be almost neglected as a possible cause of HRP staining. Possibly Amplex Red radicals are involved, which are suspected to react with surfaces when produced in a setup with a high surface-to-volume ratio [26]. Nevertheless, it was possible to stain the immobilized BSA with rhodamine 123, revealing the expected immobilization pattern (Figure 9) and proving that the inactive protein was immobilized by DEP on TiN ring electrodes.

## 5 | CONCLUDING REMARKS

HRP molecules were successfully immobilized without any chemical alteration on the surface of TiN ring electrode arrays by AC electrokinetic effects. An Amplex Red assay was used to characterize the activity of the immobi-



lized HRP on-chip. The HRP immobilize was active, but desorbed from the chip in the course of the measurements. It was possible to identify two fractions of immobilized HRP. The larger one was immobilized only temporarily and desorbed quickly in an exponential manner. This fraction is assumed to be adsorbed nonspecifically to random points on the SiO<sub>2</sub> surface or on top of the actual HRP immobilize. The other fraction of the immobilized enzyme was smaller, but lost only 6%–12% of its initial activity after each measurement. This fraction of HRP is concluded to be the permanently immobilized HRP on the electrode surface. The initial activity of the permanently immobilized enzyme equaled up to 45% of the activity that can be expected for a complete monolayer of HRP molecules on the electrodes. Regarding the inevitable effects of surface immobilization on enzyme activity and the uncontrolled orientation and packing of the molecules, this is a rather high fraction of retained activity for a surface-immobilized enzyme. The elucidation of the high residual activity of HRP after AC electrokinetic immobilization is an important step toward the application of this method in research as well as in sensing and biotechnology.

For future use of this kind of active enzyme array, the stability of the immobilize should be optimized, for example, by tuning the DEP conditions, composition of the substrate solution, and handling of the chip. The washing of the randomly adsorbed fraction of HRP could be accelerated by using a surfactant, for example, Tween 20 [45], and would be done before the actual use of the enzyme array. For single-enzyme molecule studies, active enzyme molecules would be immobilized on cone shaped silicon electrodes [16]. Tip sizes <2 nm are already available and should allow the singling of enzyme molecules as soon as a molecule with a diameter slightly larger than the tip diameter is used [17].

## ACKNOWLEDGMENTS

We thank Sandra Stanke and Marlen Kruse for helpful discussions and Emily Kroll for helping with 3D graphics. We gratefully acknowledge funding by the European Regional Development Fund (ERDF) and by the Brandenburg Ministry of Science, Research and Cultural Affairs (MWFK) within the framework StaF.



## CONFLICT OF INTEREST

The authors have declared no conflict of interest.

## DATA AVAILABILITY STATEMENT

The data that support the findings of this study are available from the corresponding author upon reasonable request.

## ORCID

Mareike Prüfer  <https://orcid.org/0000-0003-1561-1587>  
Christian Wenger  <https://orcid.org/0000-0003-3698-2635>

## REFERENCES

1. Pohl HA. Dielectrophoresis: the behavior of neutral matter in nonuniform electric fields. Cambridge, New York: Cambridge University Press; 1978.
2. Pethig R. Dielectrophoresis. Chichester, UK: John Wiley & Sons, Ltd; 2017.
3. Abd Rahman N, Ibrahim F, Yafouz B. Dielectrophoresis for biomedical sciences applications: a review. *Sensors*. 2017;17(3):449.
4. Morgan H, Hughes MP, Green NG. Separation of submicron bioparticles by dielectrophoresis. *Biophys J*. 1999;77(1):516–25.
5. Stanke S, Wenger C, Bier FF, Hölzel R. AC electrokinetic immobilization of influenza virus. *Electrophoresis*. 2022;43:1309–21.
6. Seyedi SS, Matyushov DV. Protein dielectrophoresis in solution. *J Phys Chem B*. 2018;122(39):9119–27.
7. Pethig R. Limitations of the Clausius-Mossotti function used in dielectrophoresis and electrical impedance studies of biomacromolecules. *Electrophoresis*. 2019;40:2575–83.
8. Hölzel R, Pethig R. Protein dielectrophoresis: I. status of experiments and an empirical theory. *Micromachines*. 2020;11(5):533.
9. Hayes MA. Dielectrophoresis of proteins: experimental data and evolving theory. *Anal Bioanal Chem*. 2020;412(16):3801–11.
10. Hölzel R, Pethig R. Protein dielectrophoresis: key dielectric parameters and evolving theory. *Electrophoresis*. 2021;42(5):513–38.
11. Bakewell DJG, Hughes MP, Milner JJ, Morgan H. Dielectrophoretic manipulation of avidin and DNA. In: Chang HK, Zhang Y-T, editors. *Proceedings of the 20th Annual International Conference of the IEEE Engineering in Medicine and Biology Society*, Hong Kong Sar, China, October 29–November 1, 1998. Piscataway, NJ: IEEE Service Center; 1998. p. 1079–82.
12. Hölzel R, Calander N, Chiragwandi Z, Willander M, Bier FF. Trapping single molecules by dielectrophoresis. *Phys Rev Lett*. 2005;95(12):128102.
13. Laux E-M, Kaletta UC, Bier FF, Wenger C, Hölzel R. Functionality of dielectrophoretically immobilized enzyme molecules. *Electrophoresis*. 2014;35(4):459–66.
14. Laux E-M, Wenger C, Bier FF, Hölzel R. AC electrokinetic immobilization of organic dye molecules. *Anal Bioanal Chem*. 2020;412:3859–70.
15. Yamamoto T, Fujii T. Active immobilization of biomolecules on a hybrid three-dimensional nanoelectrode by dielectrophoresis for single-biomolecule study. *Nanotechnology*. 2007;18(49):495503.
16. Wenger C, Knigge X, Fraschke M, Wolansky D, Wolff A, Mehr W, et al. Label-free Immobilization of Nano-particles on Silicon based Electrodes for Single-biomolecule Studies. In: *Proceedings of the International Conference on Biomedical Electronics and Devices (BIODEVICES-2014)*. Sebútal, Portugal: Science and Technology Publication, Lda. p. 176–80.
17. Knigge X, Wenger C, Bier FF, Hölzel R. Dielectrophoretic immobilisation of nanoparticles as isolated singles in regular arrays. *J Phys D: Appl Phys*. 2018;51(6):65308.

18. Laux E-M, Knigge X, Bier FF, Wenger C, Hölzel R. Dielectrophoretic immobilization of proteins: quantification by atomic force microscopy. *Electrophoresis*. 2015;36(17):2094–101.
19. Otto S, Kaletta U, Bier FF, Wenger C, Hölzel R. Dielectrophoretic immobilisation of antibodies on microelectrode arrays. *Lab Chip*. 2014;14(5):998–1004.
20. Berglund GI, Carlsson GH, Smith AT, Szöke H, Henriksen A, Hajdu J. The catalytic pathway of horseradish peroxidase at high resolution. *Nature*. 2002;417(6887):463–8.
21. Yang BY, Gray JSS, Montgomery R. The glycans of horseradish peroxidase. *Carbohydr Res*. 1996;287(2):203–12.
22. Veitch NC. Horseradish peroxidase: a modern view of a classic enzyme. *Phytochemistry*. 2004;65(3):249–59.
23. Edman L, Földes-Papp Z, Wennmalm S, Rigler R. The fluctuating enzyme: a single molecule approach. *Chem Phys*. 1999;247(1):11–22.
24. Hassler K, Rigler P, Blom H, Rigler R, Widengren J, Lasser T. Dynamic disorder in horseradish peroxidase observed with total internal reflection fluorescence correlation spectroscopy. *Opt Express*. 2007;15(9):5366–75.
25. Comellas-Aragonès M, Engelkamp H, Claessen VI, Sommerdijk NAJM, Rowan AE, Christensen PCM, et al. A virus-based single-enzyme nanoreactor. *Nat Nanotechnol*. 2007;2(10):635–9.
26. Gorris HH, Walt DR. Mechanistic aspects of horseradish peroxidase elucidated through single-molecule studies. *J Am Chem Soc*. 2009;131(17):6277–82.
27. Piwonski HM, Goomanovsky M, Bensimon D, Horovitz A, Haran G. Allosteric inhibition of individual enzyme molecules trapped in lipid vesicles. *Proc Natl Acad Sci U S A*. 2012;109(22):E1437–43.
28. Gao Y, Liu X, Sun L, Xu Y, Yang S, Fan C, et al. Alleviated inhibition of single enzyme in confined and crowded environment. *J Phys Chem Lett*. 2019;10(1):82–9.
29. Rodríguez-López JN, Hernández-Ruiz J, García-Cánovas F, Thorneley RN, Acosta M, Arnao MB. The inactivation and catalytic pathways of horseradish peroxidase with m-chloroperoxybenzoic acid: a spectrophotometric and transient kinetic study. *J Biol Chem*. 1997;272(9):5469–76.
30. Pace CN, Vajdos F, Fee L, Grimsley G, Gray T. How to measure and predict the molar absorption coefficient of a protein. *Protein Sci*. 1995;4(11):2411–23.
31. Ortiz de Montellano PR, David SK, Ator MA, Tew D. Mechanism-based inactivation of horseradish peroxidase by sodium azide. Formation of meso-azidoporphyrin IX. *Biochemistry*. 1988;27(15):5470–6.
32. Schneider CA, Rasband WS, Eliceiri KW. NIH Image to ImageJ: 25 years of image analysis. *Nat Methods*. 2012;9(7):671–5.
33. Nečas D, Klapetek P. Gwyddion: an open-source software for SPM data analysis. *Open Phys*. 2012;10(1):181–8.
34. Zhou M, Diwu Z, Panchuk-Voloshina N, Haugland RP. A stable nonfluorescent derivative of resorufin for the fluorometric determination of trace hydrogen peroxide: applications in detecting the activity of phagocyte NADPH oxidase and other oxidases. *Anal Biochem*. 1997;253(2):162–8.
35. Dębski D, Smulik R, Zielonka J, Michałowski B, Jakubowska M, Dębowska K, et al. Mechanism of oxidative conversion of Amplex® Red to resorufin: pulse radiolysis and enzymatic studies. *Free Radic Biol Med*. 2016;95:323–32.
36. Armbruster DA, Pry T. Limit of blank, limit of detection and limit of quantitation. *Clin Biochem Rev*. 2008;29(Suppl 1):S49–52.
37. Zhao B, Summers FA, Mason RP. Photooxidation of Amplex Red to resorufin: implications of exposing the Amplex Red assay to light. *Free Radic Biol Med*. 2012;53(5):1080–7.
38. Dai W-L, Ding J, Zhu Q, Gao R, Yang X. Tungsten containing materials as heterogeneous catalysts for green catalytic oxidation process. *Catalysis*. 2016;28:1–27.
39. Luna ML, Cedeno-Caero L. Tungsten based catalysis for oxidative desulfurization: surface species and partially reduced systems as key features to improve the activity. *J Appl Res Technol*. 2018;16:455–65.
40. Lee C-W, Chen Y-C, Ostafin A. The Accuracy of Amplex Red Assay for Hydrogen Peroxide in the Presence of Nanoparticles. *J Biomed Nanotechnol*. 2009;5(5):477–85.
41. Laberge M, Huang Q, Schweitzer-Stenner R, Fidy J. The endogenous calcium ions of horseradish peroxidase C are required to maintain the functional nonplanarity of the heme. *Biophys J*. 2003;84(4):2542–52.
42. Katchalski-Katzir E. Immobilized enzymes—learning from past successes and failures. *Trends Biotechnol*. 1993;11(11):471–8.
43. Hoarau M, Badiéyan S, Marsh ENG. Immobilized enzymes: understanding enzyme-surface interactions at the molecular level. *Org Biomol Chem*. 2017;15(45):9539–51.
44. Liu Y, Ogorzalek TL, Yang P, Schroeder MM, Marsh ENG, Chen Z. Molecular orientation of enzymes attached to surfaces through defined chemical linkages at the solid-liquid interface. *J Am Chem Soc*. 2013;135(34):12660–9.
45. Jasensky J, Ferguson K, Baria M, Zou X, McGinnis R, Kaneshiro A, et al. Simultaneous observation of the orientation and activity of surface-immobilized enzymes. *Langmuir*. 2018;34(31):9133–40.
46. Arnao MB, Acosta M, del Rio JA, Varón R, García-Cánovas F. A kinetic study on the suicide inactivation of peroxidase by hydrogen peroxide. *Biochim Biophys Acta Protein Struct Mol Enzym*. 1990;1041(1):43–7.
47. Hernández-Ruiz J, Arnao MB, Hiner ANP, García-Cánovas F, Acosta M. Catalase-like activity of horseradish peroxidase: relationship to enzyme inactivation by H<sub>2</sub>O<sub>2</sub>. *Biochem J*. 2001;354(1):107–14.
48. Stanke S, Bier FF, Hölzel R. Fluid streaming above interdigitated electrodes in dielectrophoresis experiments. *Electrophoresis*. 2011;32(18):2448–55.

## SUPPORTING INFORMATION

Additional supporting information can be found online in the Supporting Information section at the end of this article.

**How to cite this article:** Prüfer M, Wenger C, Bier FF, Laux E-M, Hölzel R. Activity of AC electrokinetically immobilized horseradish peroxidase. *Electrophoresis*. 2022;1–14. <https://doi.org/10.1002/elps.202200073>